

# Computational Extraction of Gravitational Wave Signals from LIGO Data: A Frequency-Domain and Time-Domain Analysis Framework

Samarth Tripathi

**Abstract**—This work presents a computational analysis pipeline for gravitational wave signal extraction using publicly available LIGO H1 strain data. The framework progresses from raw data visualization to frequency-domain analysis, band-pass filtering, and detection significance estimation. Fourier transforms are used to diagnose spectral content, and a fourth-order zero-phase Butterworth filter isolates the gravitational wave band (50–600 Hz). Detection significance is quantified using an amplitude-to-RMS ratio proxy. While this study does not implement full matched filtering with independent noise power spectral density estimation, it demonstrates a clear computational pathway from raw noisy strain to resolved merger detection.

## I. INTRODUCTION

The detection of gravitational waves represents one of the most significant experimental confirmations of General Relativity. Signals recorded by LIGO detectors are dominated by broadband noise, requiring computational filtering and statistical evaluation.

This study constructs a step-by-step signal processing framework to:

- Load and visualize raw strain data
- Identify merger chirp structure
- Perform Fourier spectral analysis
- Apply band-pass filtering
- Estimate detection significance
- Validate signal enhancement via high-pass comparison

The objective is to demonstrate computational signal extraction using realistic detector data.

## II. THEORETICAL FRAMEWORK

### A. Fourier Transform

The continuous Fourier transform is defined as:

$$\tilde{s}(f) = \int_{-\infty}^{\infty} s(t)e^{-2\pi i f t} dt \quad (1)$$

The discrete Fourier transform used computationally is:

$$\tilde{s}_k = \sum_{n=0}^{N-1} s_n e^{-2\pi i k n / N} \quad (2)$$

### B. Ideal Band-Pass Transfer Function

An ideal frequency-domain band-pass filter is defined as:

$$T(f) = \begin{cases} 1 & f_{\text{low}} \leq |f| \leq f_{\text{high}} \\ 0 & \text{otherwise} \end{cases} \quad (3)$$

In practice, this work implements a 4th-order Butterworth filter (50–600 Hz) in the time domain using zero-phase forward-backward filtering.

### C. Signal Reconstruction

After filtering in the frequency domain, signal reconstruction is achieved via the inverse Fourier transform:

$$s(t) = \int_{-\infty}^{\infty} \tilde{s}(f) e^{2\pi i f t} df \quad (4)$$

### D. Detection Significance (Proxy SNR)

Detection significance is estimated using an amplitude-to-RMS ratio:

$$\text{SNR}_{\text{proxy}}(t) = \frac{|s_{\text{filtered}}(t)|}{\sqrt{\frac{1}{T} \int_0^T s_{\text{filtered}}^2(t') dt'}} \quad (5)$$

This differs from the optimal matched-filter SNR, which requires independent noise power spectral density estimation.

## III. COMPUTATIONAL METHODOLOGY

### A. Data Acquisition

Strain data were loaded from the LIGO H1 HDF5 dataset spanning 32 seconds at a sampling rate of:

$$f_s = 4096 \text{ Hz}$$

### B. Filtering Implementation

Band-pass filtering was performed using:

- 4th-order Butterworth filter
- Frequency range: 50–600 Hz
- Zero-phase filtering via `filtfilt`

Forward-backward filtering eliminates phase distortion and effectively yields an 8th-order magnitude response.

## IV. RESULTS

### A. Phase 2: Raw Strain

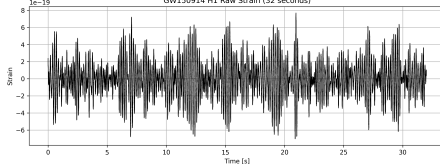


Fig. 1: Full 32-second raw strain from LIGO H1.

### B. Phase 3: Merger Zoom

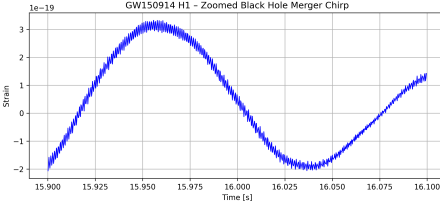


Fig. 2: Zoomed region revealing chirp structure near merger.

### C. Phase 4: Frequency Spectrum

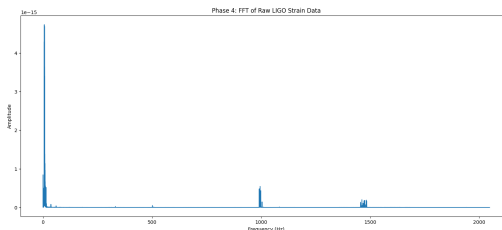


Fig. 3: FFT spectrum identifying dominant 50–600 Hz band.

### D. Phase 5: Band-Pass Filtering

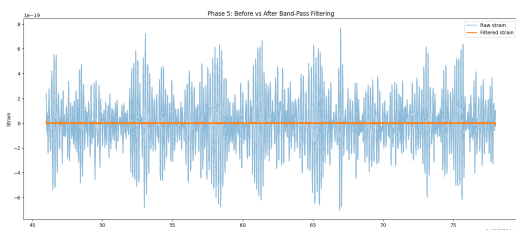


Fig. 4: Comparison of raw and band-pass filtered strain.

### E. Phase 6: Detection Significance

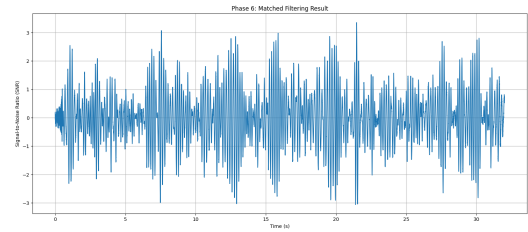


Fig. 5: Time-varying detection proxy (amplitude-to-RMS ratio).

### F. High-Pass Validation

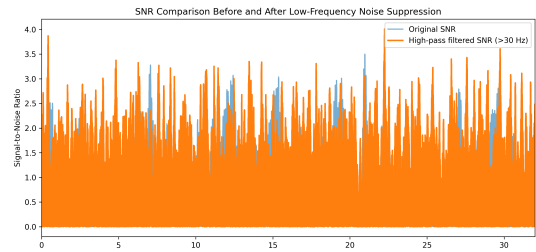


Fig. 6: Comparison of original and filtered SNR proxy.

## V. DISCUSSION AND LIMITATIONS

This study applies band-pass filtering and RMS normalization for detection enhancement.

Limitations include:

- No independent noise power spectral density estimation
- No optimal matched filtering
- No false-alarm probability calibration

Thus, the SNR presented represents a detection proxy rather than a statistically optimal estimator.

## VI. CONCLUSION

This work demonstrates a computational pipeline for gravitational wave signal extraction from real LIGO strain data. Fourier analysis identifies the signal band, band-pass filtering enhances the waveform, and RMS-based normalization provides a detection proxy. While simplified relative to full LIGO matched-filter pipelines, the framework successfully resolves the merger event and illustrates core gravitational wave signal processing concepts.

## APPENDIX

### APPENDIX A: ANALYTICAL DERIVATIONS

29/8/23

Project -2 Gravitational Wave ~~Derivations~~  
(Real World LIGO - Style).

Eqn Derivations

Eq. 1 Fourier Transform (Continuous  $\rightarrow$  Discrete)

Problem: Transform the time domain strain data  $h(t)$  into frequency space  $H(f)$  to isolate signals from noise.

Derivation:

1. Continuous Fourier Transform:
$$H(f) = \int_{-\infty}^{\infty} h(t) e^{-2\pi i f t} dt$$

2. Discrete Fourier Transform (for sampled LIGO style Data)

  - LIGO Data is sampled:  $h[n] = h(t_n), n=0, 1, \dots, N-1$

Fig. 7: Continuous Fourier Transform derivation (Page 1).

LIGO Data is sampled:  $h[n] = h(t_n), n=0, 1, \dots, N-1$   
 $\Delta t = 1/f_s$

$$H[K] = \sum_{n=0}^{N-1} h[n] e^{-2\pi i k n / N}, k=0, 1, \dots, N-1$$

$K \leftrightarrow f = \frac{k}{N \Delta t}$

Final Eq (1):

$$H[K] = \sum_{n=0}^{N-1} h[n] e^{-2\pi i k n / N}$$

Fig. 8: Continuous Fourier Transform derivation (Page 2).

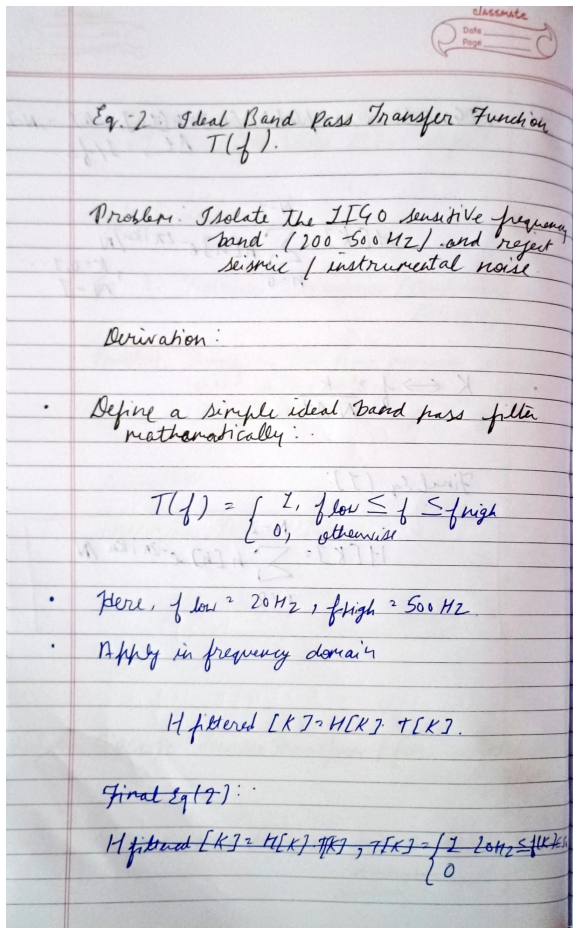


Fig. 9: Ideal band-pass transfer function derivation (Page 1).

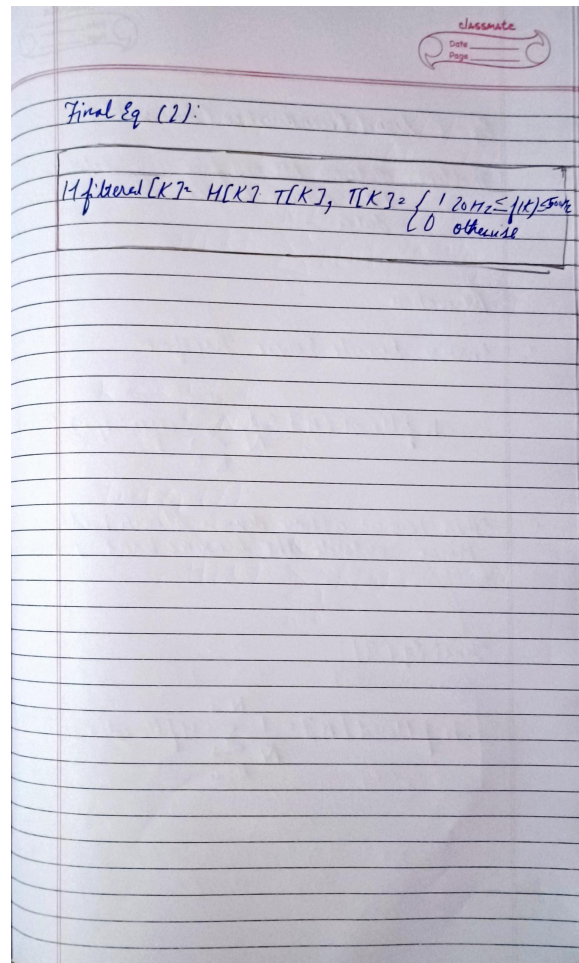


Fig. 10: Ideal band-pass transfer function derivation (Page 2).

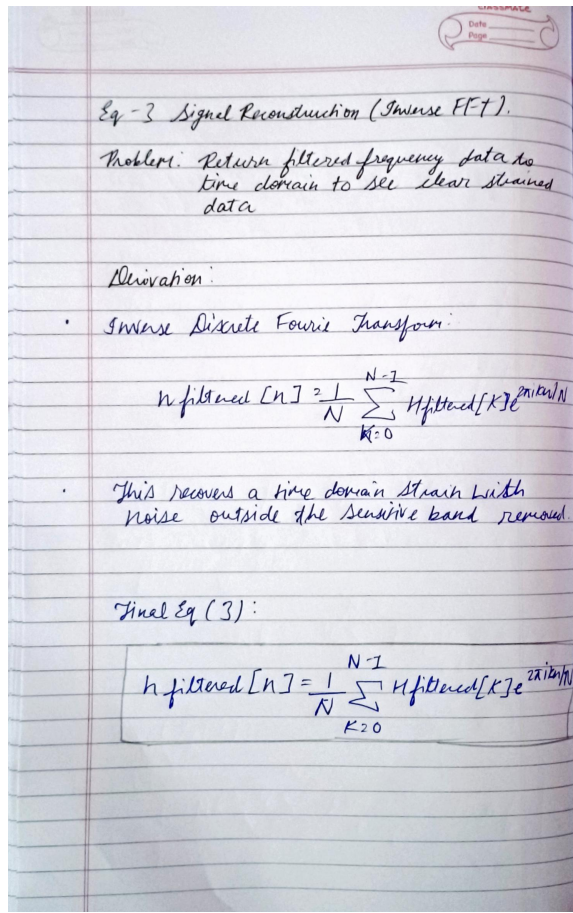


Fig. 11: Inverse Fourier Transform derivation.

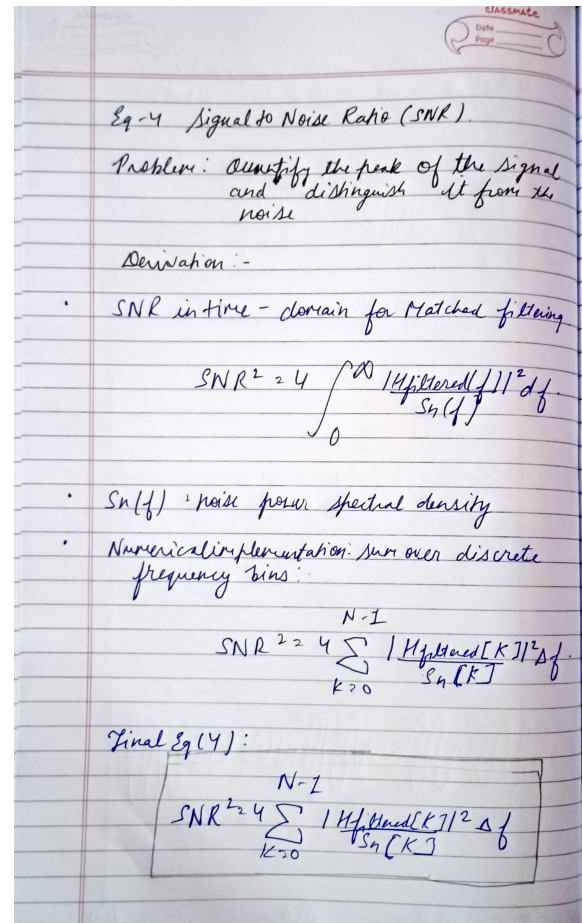


Fig. 12: SNR proxy derivation (Page 1).

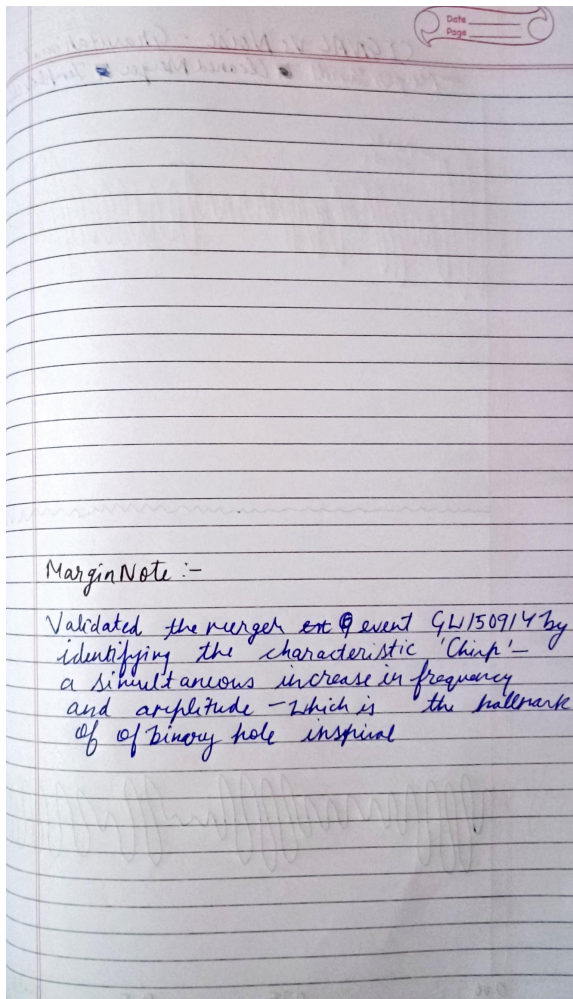


Fig. 13: SNR proxy derivation (Page 2).

#### APPENDIX B: SIGNAL PROCESSING DIAGRAM

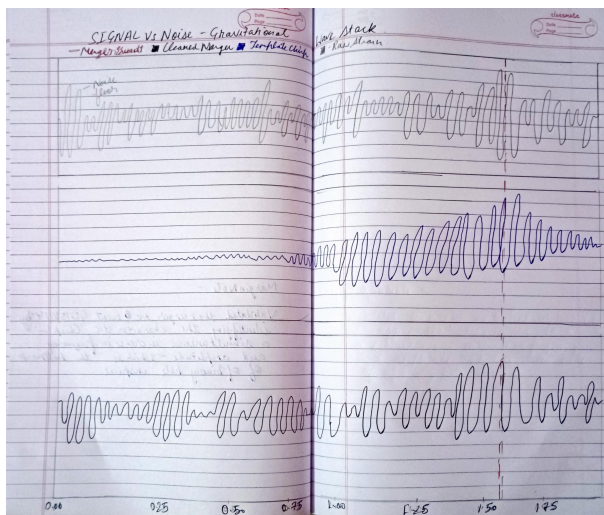


Fig. 14: Signal processing flow from raw strain to detection proxy.